Supplementary Information

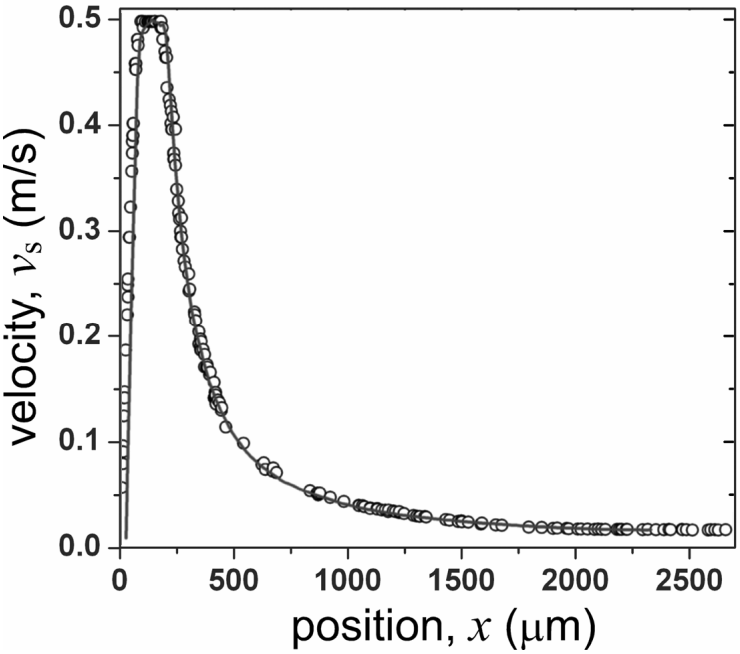

Figure S-1. Velocity of the 3D-focused stream, v_s, as a function of the position along the main channel, *x*, at the maximal flow velocity $v_{\max} = 0.5$ m/s. The velocity was measured by the tracking of fluorescent particles in the focused stream (symbols) and calculated using 3D numerical simulations in FEMLAB (continuous line). The time of passage of the sample through the observation channel, t_{ob}, from its beginning at $x = x_0 = 200$ μm to the last point at $x = x_1 = 2650$ μm, was calculated by numerical integration of the velocity data as $t_{ob} = \int_{x_0}^{x_1} \frac{dx}{v_s(x)} \approx 90$ ms. Under an assumption that the flow velocity in the observation channel (where the Reynolds number is always relatively low and the flow is expected to be nearly linear) changes proportionally to $v_{\max}$, the passage time can be generally expressed as $t_{ob} = \frac{45\,\text{mm}}{v_{\max}}$.

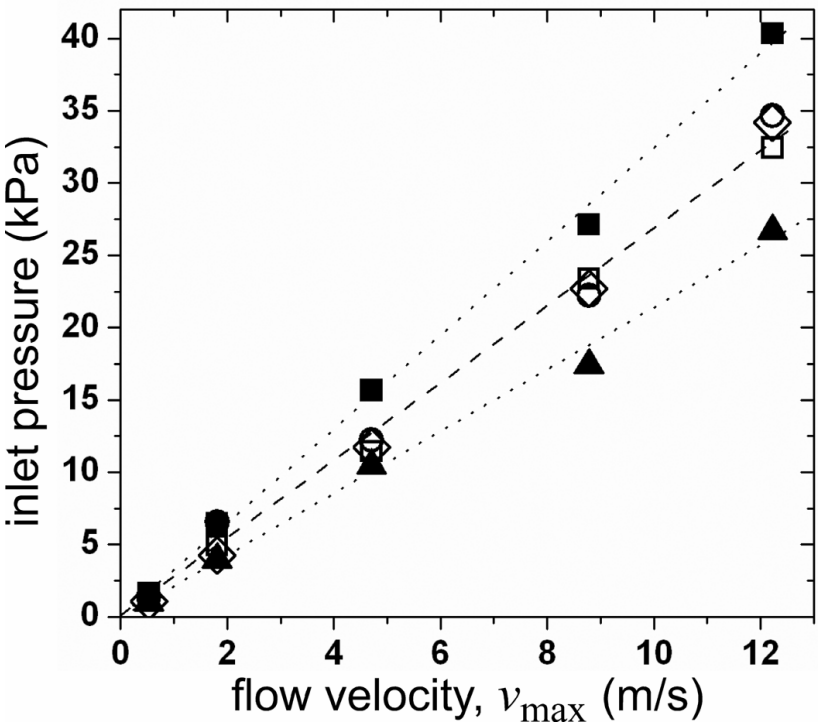

Figure S-2. Differential pressures at the devices inlets *A* (open circles), *B* (solid triangles), *C* (open squares), *D* (open diamonds), and *E* (solid squares) at different maximal flow velocities, v_{max}, that were used in the experiments.

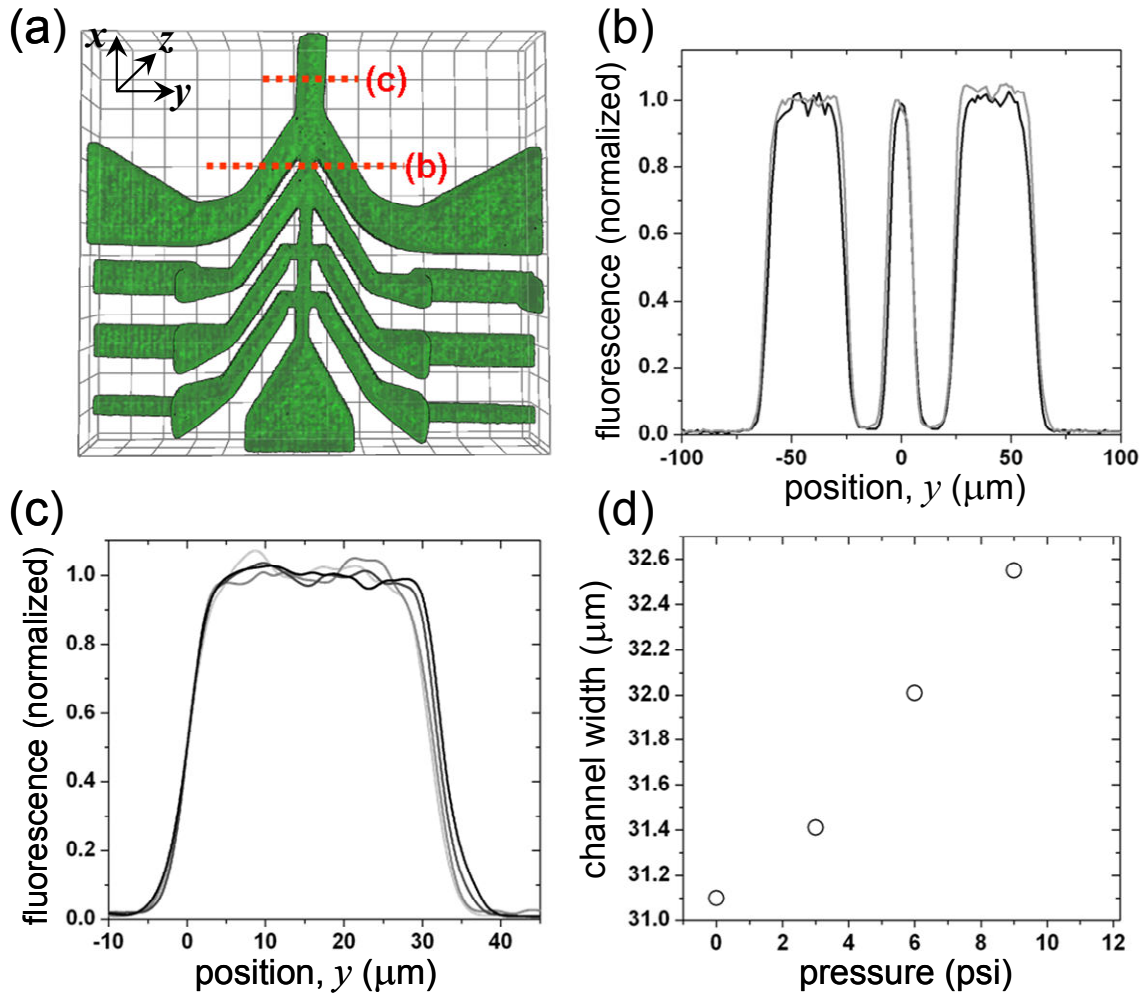

Figure S-3. Deformation of channels in the microfluidic device under pressure. The device was filled with a 10 ppm (by weight) solution of fluorescein, the outlet was connected to a source of compressed air with regulated pressure, and all other ports of the device were blocked, rendering pressure everywhere in the device equal to pressure at the outlet. To evaluate deformations of channel side walls, fluorescence micrographs of the region with the 3D flow focusing element and the mixing channel were taken using a spinning disk confocal microscope. **(a)** 3D reconstruction of the imaging area (with the 3D focusing element at the bottom and the mixing channel at the top) obtained by stacking individual confocal scans. **(b)** and **(c)** y-axis distributions of normalized fluorescence from scans taken at the mid-plane of the channels (27.5 μm from the bottom) at the positions marked by dashed lines (b) and (c), respectively, in panel (a). Grey and black curves in (b) correspond to pressures of 0 and 9 psi (62 kPa), respectively. The central peak in (b) corresponds to the injection channel. Curves in (c) show fluorescence in the mixing channel at pressures of 0, 3, 6, and 9 psi. Curves in darker gray correspond to higher pressures. The position $y = 0$ corresponds to a

normalized fluorescence of 0.5 (the putative location of the left wall of the channel) for all curves. **(d)** Width of the mixing channel, which is calculated as the full width at half height of the curves in panel (c), as a function of pressure. At a pressure of 6 psi (41 kPa), which is the pressure applied to inlet *E* of the device in the experiment with the highest flow velocity ($v_{\max} = 12$ m/s, Supplementary Information, Fig. S-2), the width of the mixing channel is increased by 0.9 μm. A 2D numerical simulation in FEMLAB (not shown) for a channel with a cross-section of 31×55 μm (as the mixing channel) with a uniform pressure of 41 kPa applied to all channel walls and with no displacement at the PDMS-glass interface (at the bottom of the side walls) indicated that the 0.9 μm increase of the channel width at the mid-plane corresponds to PDMS with a Young's modulus of 4 MPa (at the Poisson ratio of 0.5 of PDMS).